DNA-Templated Assembly of Conducting Gold Nanowires between Gold Electrodes on a Silicon Oxide Substrate

Andrea Ongaro,[†] Fionn Griffin,[†] Paul Beecher,[‡] Lorraine Nagle,[†] Daniela Iacopino,[†] Aidan Quinn,[‡] Gareth Redmond,[‡] and Donald Fitzmaurice*,[†]

Department of Chemistry, University College Dublin, Belfield, Dublin 4, Ireland, and NMRC, University College Cork, Lee Maltings, Cork, Ireland

Received November 21, 2004. Revised Manuscript Received February 8, 2005

Here we report on the DNA-templated self-assembly of conducting gold nanowires between gold electrodes lithographically patterned on a silicon oxide substrate. An aqueous dispersion of 4-(dimethylamino)pyridine-stabilized gold nanoparticles was prepared. These nanoparticles recognize and bind selectively double-stranded calf thymus DNA aligned between the gold electrodes to form a linear nanoparticle array. Continuous polycrystalline gold nanowires are obtained by electroless deposition that enlarges and enjoins the individual gold nanoparticles. The above nanowires were structurally characterized using a range of electron and scanning probe microscopies and electrically characterized at room temperature using a standard probe setup. The results of these characterizations show these wires to be 20 nm high and 40 nm wide, to be continuous between interdigitated gold electrodes with an interelectrode spacing of 0.2 or 1.0 μm, and to possess a resistivity of 2×10^{-4} Ωm. These DNA-templated nanowires, the smallest reported to date, exhibit resistivities consistent with reported findings and current theory. The use of DNA as a template for the self-assembly of conducting gold nanowires represents a potentially important approach to the fabrication of nanoscale interconnects.

Introduction

The demand for integrated circuits that will allow information to be retrieved, processed, and stored at even faster speeds remains undiminished. This is despite the fact that scaling has doubled the density of the wires and switches that comprise such circuits every 18 months giving rise to Moore's Law.[1] While it is expected that Moore's Law will continue to hold true until 2012, it is not expected that it will hold true thereafter.[2]

In order for Moore's Law to hold true until 2012, major advances in existing fabrication and materials technologies will be required. Specifically, the development of new short-wavelength light sources, masks and resists, and materials with high and low dielectric constants. The engineering and scientific advances, not to mention the investment that will be required to securing these advances, are very significant.

Even assuming these challenges are met, the sizes of the wires and switches that comprise the integrated circuits of the future will be so small that the materials from which they are fabricated will no longer exhibit bulk properties. Instead, these materials will exhibit properties that are dominated by surface and confinement effects. For these reasons, it is necessary to contemplate alternative fabrication technologies and new processor architectures, which can accommodate or even exploit the novel properties exhibited by nanoscale components.

When considering alternative fabrication technologies, one is immediately attracted to the self-assembly in solution and the self-organization at technologically relevant substrates of functional nanoscale architectures.[3] When considering alternative materials technologies, one is immediately attracted to high information content molecules and nanoparticles.[4,5] There have been a number of recent reports that have demonstrated the potential of these and related approaches to developing alternative fabrication technologies.[6−10]

An important goal will be the use of high information content molecules and nanoparticles to self-assemble and self-organize nanowire interconnects in solution and at lithographically patterned silicon oxide substrates, respectively.[11] For example, it has been shown that the electrostatic interaction between DNA and suitably charged metal and semiconductor nanoparticles can result in the ordering of these nanoparticles as linear arrays.[12] In some cases, transport properties have been measured for these arrays.[13]

* To whom correspondence should be addressed. E-mail: donald.fitzmaurice@ucd.ie.
† University College Dublin.
‡ University College Cork.

(1) Moore, G. E. *Electronics* **1965**, *38*.
(2) International Technology Roadmap for Semiconductors, 2002, http:// public.itrs.net/.
(3) Parviz, B.; Ryan, D.; Whitesides, G. *IEEE Trans. Adv. Pac.* **2003**, *26*, 233.
(4) Niemeyer, C. *Angew. Chem., Int. Ed.* **2001**, *40*, 4128.
(5) Parak, W.; Gerion, D.; Pellegrino, T.; Zanchet, D.; Micheel, C.; Williams, S.; Boudreau, R.; Le Gros, M.; Larabell, C.; Alivisatos, P. *Nanotechnology* **2003**, *14*, 15.
(6) Braun, E.; Eichem, Y.; Sivan, U.; Ben-Yoseph, G. *Nature* **1998**, *391*, 775.
(7) Collier, C.; Wong, E.; Belohradsky, M.; Raymo, F.; Stoddart, F.; Kuekes, P.; Williams, R.; Heath, J. *Science* **1999**, *285*, 391.
(8) Keren, K.; Krueger, M.; Gilad, R.; Ben-Yoseph, G.; Sivan, U.; Braun, E. *Science* **2002**, *297*, 72.
(9) Yan, H.; Park, S.; Finkelstein, G.; Reif, J.; La Bean, T. *Science* **2003**, *301*, 1882.
(10) Xin, H.; Woolley, A. *J. Am. Chem. Soc.* **2003**, *125*, 8710.
(11) Richter, J. *Physica E* **2003**, *16*, 157.

10.1021/cm047970w CCC: $30.25
Published on Web 03/19/2005

It is in this context that we report that 4-nm diameter 4-(dimethylamino) pyridine (DMAP)-modified gold nanoparticles recognize and bind selectively double-stranded calf thymus DNA. We also report that, as a consequence, it is possible to use double-stranded calf thymus DNA to template the self-assembly of gold nanowires between gold electrodes conventionally patterned on a silicon wafer substrate. Subsequent structural and electronic characterization of these wires established their dimensions and allowed their resistivities to be measured. These findings provided insights in to the relative magnitudes of the contributions of electron scattering at the contacts and within the nanowire to the measured resistivities.

Experimental Section

Preparation of Gold Nanoparticles. A stable aqueous dispersion of DMAP-stabilized gold nanoparticles was prepared as described in detail elsewhere.[14] Briefly, DMAP was transferred from a chloroformic phase to an aqueous phase containing hydrochloroauric acid. Subsequent reduction, by the addition of sodium borohydride, led to nanoparticle formation. The nanoparticles were characterized by transmission electron microscopy (TEM) and were found to have an average diameter of 3.6 nm and polydispersity of 1.10 . The nanoparticle concentration of the as-prepared dispersion was 17.6 μM. Prior to use, 10 μL of the above dispersion was diluted in 1 mL of water yielding a nanoparticle concentration of 176 nM at pH 8.0.

To characterize the interaction between the above DMAP-modified gold nanoparticles and the DNA−biotin template, gel electrophoresis and microelectrophoresis studies were undertaken. Gel electrophoresis was performed in a 2% agarose gel matrix. The DMAP-modified gold nanoparticles were observed to migrate to the negative electrode, indicating a net positive charge on the nanoparticles.

Microelectrophoresis studies were performed using a Malvern Zetasizer 3000 HSA. The Zeta potential was calculated using the Smoluchowski approximation. An average value of +23.5 mV was measured for a 176 nM dispersion of DMAP-modified gold nanoparticles at pH 8.0. This value confirms both the stability of the nanoparticles and net overall positive charge at the radius of shear.

The above measurements indicate that the interaction between the DNA template and the DMAP-modified gold nanoparticles is mainly electrostatic, with the negatively charged backbone of the DNA template attracting the positively charged DMAP-modified gold nanoparticles.

Preparation of Calf Thymus DNA. Double-stranded calf thymus DNA (SIGMA) was diluted in tris-EDTA buffer (pH 7.4) to yield a concentration of 500 ng/μL. This solution was subsequently diluted to 20 ng/μL and stored at 4 °C until required for use.

Polylysine-Modified Carbon-Coated Copper TEM Grid Substrates. DNA samples were deposited on carbon-coated 400 mesh copper TEM grids, which had previously been modified by depositing an aliquot (20 μL) of polylysine solution (5 μg/mL) on the carbon-coated substrate. This served to increase the hydrophilicity of the carbon surface and to improve DNA binding.

Bare Plasma-Treated Silicon Wafer Substrates. Silicon wafers (n-type, 2−4 Ω cm) were heated to 350 °C in air for 4 h, cleaned using a piranha solution (70% H_2SO_4, 30% H_2O_2), and stored under ethanol until required for use. Immediately prior to use they were cleaned again using oxygen plasma (30 W, 50 Hz, 0.2−0.8 mbar O_2) for 5 min.

Lithographically Patterned Plasma-Treated Silicon Oxide Substrates. Interdigitated electrodes with an interelectrode spacing of 0.2 or 1.0 μm were fabricated on an oxidized silicon wafer (*n*-Si, 500-nm thermal oxide) substrate using electron-beam lithography, metal evaporation (Ti 2 nm, Au 20 nm), and lift-off. The above wafers were rinsed with acetone and 2-propanol and stored in air until required for use. Immediately prior to use they were oxygen plasma cleaned (30 W, 50 Hz, 0.2−0.8 mbar O_2) for 5 min.

Assembly of Gold Nanowires on Polylysine-Modified Carbon-Coated TEM Grids. Samples for imaging were prepared by depositing an aliquot (20 μL) of the double-stranded calf thymus DNA solution (20 ng/μL) onto the polylysine-modified carbon-coated copper grid. After 2 min, the excess solution was removed from the grid by wicking. The grid was then washed with an aliquot (20 μL) of distilled−deionized water (18.2 MΩ cm) with the consequent elongation of the DNA wires and dried in air. The double-stranded calf thymus DNA immobilized on the carbon-coated copper grids was partially metallized. An aliquot (20 μL) of the DMAP-modified gold nanoparticle dispersion (176 nM in particle at pH 8.0) was deposited on the carbon film. After 1 min, wicking was used to remove excess gold nanoparticles, and the grid was once more washed with distilled−deionized water (18.2 MΩ cm). To complete metallization of the DNA, Goldenhance solution was used. Once the DNA was deposited and metallized on a carbon-coated copper grid, the enhancement procedure followed that given by Nanoprobes (Cat. No. 2112). An incubation time of 1 min was employed.

Templated Assembly of Gold Nanowires on Plasma-Treated Bare and Lithographically Patterned Silicon Wafer Substrates. An aliquot (20 μL) of double-stranded calf thymus DNA solution (20 ng/μL) was deposited on a cleaned and plasma-treated silicon wafer substrate. The DNA solution was allowed to stand on the wafer substrate for 2 min. The deposited DNA was subsequently elongated and stretched by spinning the substrate at 1000 rpm for 10 s. Excess DNA solution was removed by spinning the substrate at 5000 rpm for about 30 s. The DNA strands were next partially metallized by depositing an aliquot (20 μL) of the DMAP-modified gold nanoparticle dispersion (176 nM in particle at pH 8.0) on the substrate. After 1 min, wicking was used to remove excess gold nanoparticles, and the grid was once more washed with distilled−deionized water (18.2 MΩ cm). To complete metallization of the DNA, Goldenhance solution was used. Once the DNA was deposited and partially metallized, the enhancement procedure followed was that given by Nanoprobes (Cat. No. 2112). An incubation time of 5 min was employed.

The same protocol was used for DNA deposition and metallization on silicon wafer substrates patterned with gold electrodes. The only exception being that an enhancement incubation time of 1 min was used.

TEM. All TEM images were recorded using a JEOL JEL-2000 EX electron microscope with a lattice resolution of 0.14 nm and a point-to-point resolution of 0.3 nm operating at 80 kV.

(12) (a) Torimoto, T.; Yamashita, M.; Kuwabata, S.; Sakata, T.; Mori, H.; Yoneyama, H. *J. Phys. Chem. B* **1999**, *103*, 8799. (b) Sastry, M.; Kumar, A.; Datar, S.; Dharmadhikari, C.; Ganesh, K. *Appl. Phys. Lett.* **2001**, *78*, 2943. (c) Warner, M.; Hutchison, J. *Nature Mater.* **2003**, *2*, 272. (d) Wang, G.; Royce, M. *Nano Lett.* **2004**, *4*, 95.

(13) Wybourne, M.; Hutchison, J.; Clarke, L.; Brown, L.; Mooster, J. *Microelectron. Eng.* **1999**, *47*, 55. (b) Berven, C.; Clarke, L.; Mooster, J.; Wybourne, M.; Hutchison, J. *Adv. Mater.* **2001**, *13*, 109. (c) Berven, C.; Wybourne, M.; Clarke, L.; Longstreth, L.; Hutchison, J.; Mooster, J. *J. Appl. Phys.* **2002**, *92*, 4513.

(14) Griffin, F.; Fitzmaurice, D. *Langmuir* **2005**, manuscript in preparation.

Atomic Force Microscopy (AFM). All AFM images were obtained using a Digital Instrument's Multimode Nanoscope III instrument, equipped with tapping mode etched silicon tips with reflex coating (Nanosensors NCHR: force constant 42 Nm^{-1}, resonant frequency 300 kHz, radius 10 nm). Images were post-processed using Nanoscope Image Software (Ver. 4.23r6).

Scanning Electron Microscopy (SEM). The SEM images were acquired using a JEOL 6700 FE-SEM operating at 10 kV.

Conductivity Measurements. The room-temperature current−voltage characteristics of the above nanowires were measured using a Hewlett-Packard 4156A parameter analyzer system on devices probed using a Wentworth PML8000 probe station.

Results

DNA Templated Assembly of Gold Nanowires on a Bare Plasma-Treated Silicon Wafer and a Polylysine-Modified Carbon-Coated Copper TEM Grid.

A drop of the DNA template solution was deposited on a plasma-treated silicon wafer substrate. Subsequent spin coating elongated the DNA template. Plasma treatment improved the binding of the DNA template to the oxide layer. Shown in Figure 1a is an AFM image of the elongated and immobilized DNA template on a silicon wafer substrate.

After elongation and immobilization of the DNA template on the above substrate, a drop of the DMAP-modified gold nanoparticle dispersion was deposited on the silicon wafer substrate. Zeta potential measurement established that these nanoparticles were positively charged. As a consequence, adsorption was selective and immediate at the negatively charged backbone of the DNA template and an exposure time of 1 min sufficed. Shown in Figure 1b is an AFM image of the partially metallized DNA template on a silicon wafer substrate.

A drop of the DNA template solution was deposited on a polylysine-modified carbon-coated TEM grid. Subsequent washing with water elongated the DNA template. Polylysine modification improved the binding of the DNA template to the carbon layer.

Following elongation and immobilization of the DNA template on the above substrate, a drop of the DMAP-modified gold nanoparticle dispersion was deposited on the carbon-coated TEM grid. As above, adsorption was selective and immediate, and an exposure time of 1 min sufficed. Shown in Figure 2a is a TEM image of the partially metallized DNA template elongated and immobilized on a carbon-coated TEM grid.

It is clear from the TEM image in Figure 2a that the DMAP-modified gold nanoparticles adsorbed at the DNA template do not form a continuous wire. This is not an unexpected finding in light of the fact that positively charged gold nanoparticles will repel each other but does serve to make clear the limitations of AFM in respect of structural characterization on this scale. Specifically, it could be mistakenly concluded from the AFM image in Figure 1b that the self-assembly of a continuous nanowire has been templated, whereas from the corresponding TEM image in Figure 2a, this is clearly not the case. This apparent discrepancy is accounted for by the fact that the scanning probe of the AFM consists of a tip with an apex diameter in the range of 5−10 nm. Since the dimension of the gaps between the gold nanoparticles adsorbed at the DNA and the scanning tip are smaller, the AFM image appears to show a continuous nanowire.

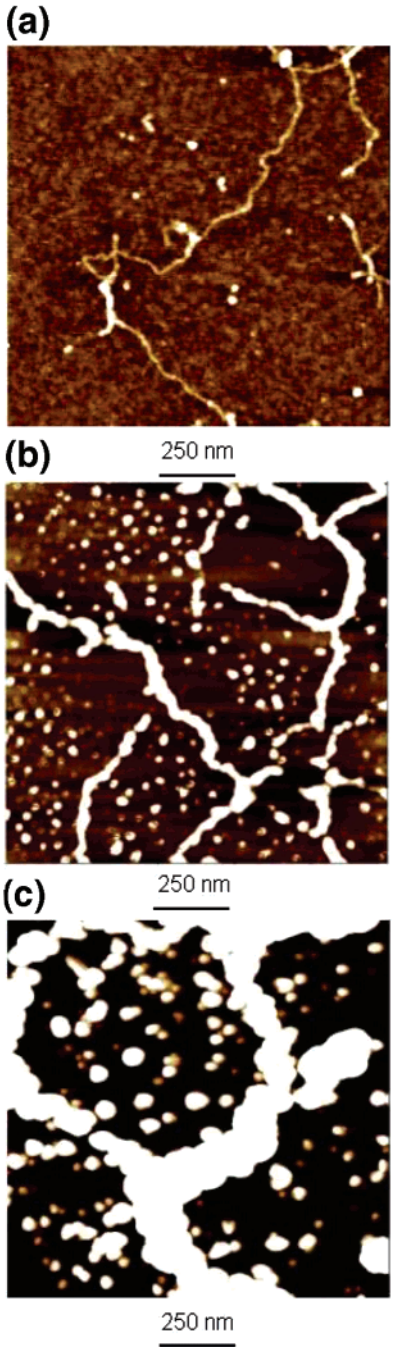

Figure 1. (a) AFM image of double-stranded calf thymus DNA elongated and immobilized on a plasma-treated silicon wafer substrate. (b) AFM image following treatment with an aqueous dispersion of DMAP-stabilized gold nanoparticles for 1 min. (c) AFM image following enlargement of the gold nanoparticles by electroless deposition for 5 min.

For these reasons, the above partially metallized DNA templates were exposed to a solution that causes the adsorbed gold nanoparticles to be enlarged and enjoined to form a continuous polycrystalline nanowire. Specifically partially metallized DNA templates on silicon wafer and carbon-coated TEM grid substrates were exposed to an electroless deposition solution for 5 and 1 min, respectively. The gold nanoparticles adsorbed at the partially metallized DNA template act as sites for the selective deposition of gold and

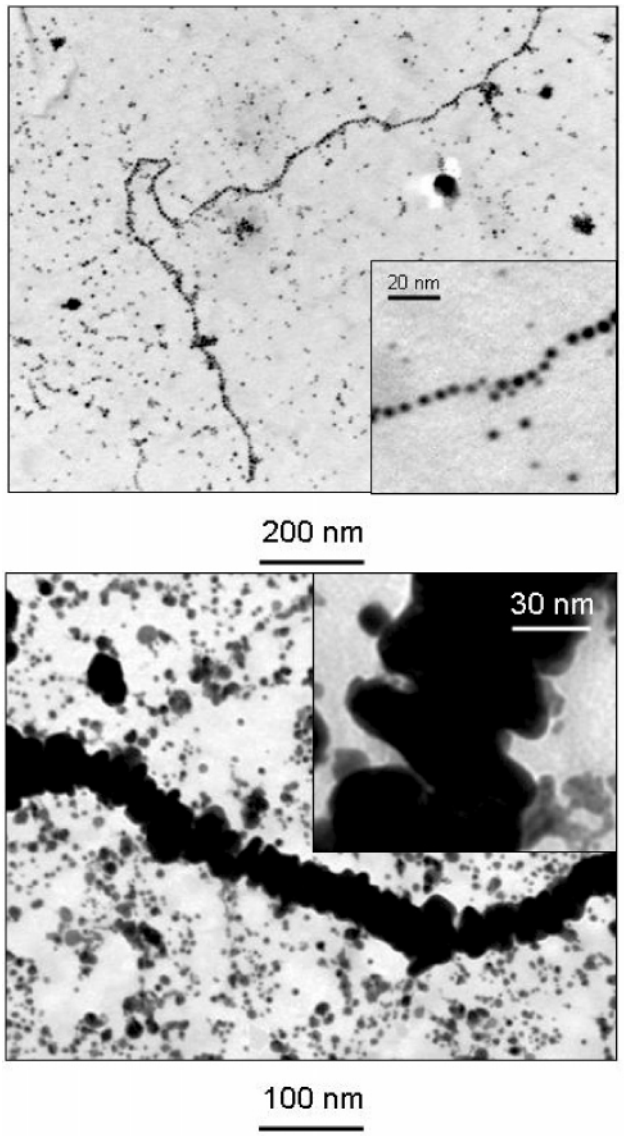

Figure 2. (a) TEM image of double-stranded calf thymus DNA immobilized on a polylysine-modified carbon-coated copper grid and treated with an aqueous dispersion of DMAP-stabilized gold nanoparticles for 1 min. (b) TEM image following enlargement of the gold nanoparticles by electroless deposition for 1 min.

are enlarged. As a result, these gold nanoparticles are enjoined and form a continuous polycrystalline gold nanowire. The diameter of the nanowire formed depends on the exposure time. AFM and TEM images show the formation of continuous polycrystalline nanowires; see Figures 1c and 2b and discussion below.

DNA-Templated Assembly of Gold Nanowires between Gold Electrodes on a Plasma-Treated Silicon Wafer and Their Electrical Characterization. Next we consider the DNA-templated assembly of gold nanowires between gold electrodes on a plasma-treated silicon wafer and their electrical characterization.

The elongation and immobilization of the double-stranded calf thymus DNA template, the selective adsorption of DMAP-modified gold nanoparticles, and the enlargement of these nanoparticles to form a continuous polycrystalline gold nanowire were all as described above for the bare silicon wafer substrate, the sole exception being that the partially

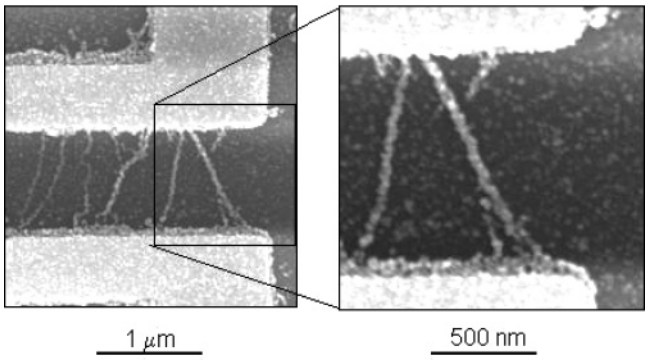

Figure 3. SEM image of a network of gold nanowires (prepared as in Figure 1 but with a shorter enhancement time of 1 min) self-assembled between parallel 1 μm gold electrodes.

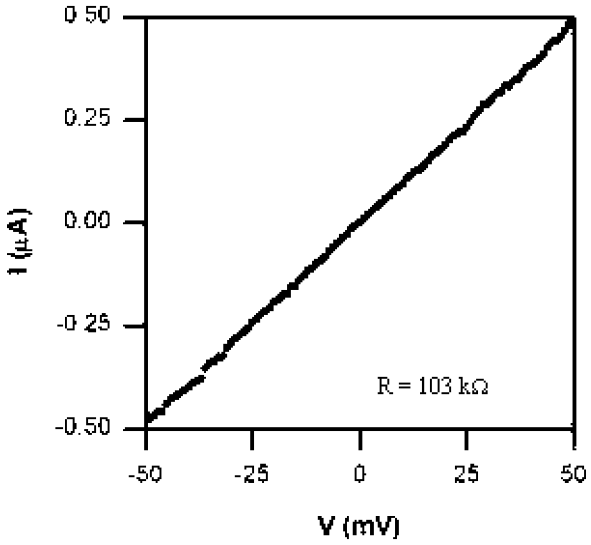

Figure 4. Plot of current vs voltage at room temperature for a network of gold nanowires assembled between the parallel 1 μm gold electrodes in Figure 3. These nanowires exhibit linear ohmic behavior and an overall resistance of 103 kΩ.

metallized DNA template was exposed to an electroless deposition solution for 1 min.

Shown in Figure 3 are SEM images of one such electrode after all of the above steps were completed. These images confirm the templated assembly of a network of nanowires across the 1.0 μm gap between alternate electrodes. It should be noted that these wires have been assembled on top of the previously deposited gold electrodes.

While these findings are potentially significant, their actual significance depends on how well the templated gold nanowires conduct current. Accordingly, two-terminal current−voltage measurements were made for the above network of nanowires. Contacting the two electrodes shown in Figure 3 yields the linear ohmic relationship shown in Figure 4, with an overall resistance of 103 kΩ.

The dimensions of the nanowires in Figure 3 were obtained from analysis of AFM images used to measure wire heights and SEM images used to measure wire diameters and lengths. The mean height was found to be 20 nm, the mean width was found to be 40 nmm and the mean length was found to be 1.25 μm. The number of nanowires contributing to charge transport (between 1 and 6) was obtained from analysis of the SEM images.

By assumption that three wires conduct, an order-of-magnitude estimate for the resistivity of a single wire is 10^{-4} Ω m, i.e., 4 orders of magnitude larger than the resistivity of bulk gold (2×10^{-8} Ω m).[15]

It should be noted that a series of related control experiments were performed. It was found that the resistivity of a plasma-treated silicon wafer patterned with gold electrodes is in the GΩ range. Similar values were obtained following deposition of the DNA template and following partial metallization of the DNA template by adsorption of DMAP-modified gold nanoparticles. Furthermore, it has been established that following enhancement of the gold nanoparticles that the measured resistivity remains in the GΩ range unless a continuous wire is formed that interconnects two electrodes. This assertion is based on a detailed analysis of numerous samples by SEM and AFM.

Discussion

We consider four contributions to the measured resistances, which together can account for the resistivities of the DNA-templated gold nanowires prepared by ourselves and by others.[8,16−18]

First, there is a contribution to the measured resistance due to electron scattering at the contacts between the gold nanowire and the electrodes. To the best of our knowledge, there are no reports to date that quantify the magnitude of this contribution to the measured resistance in DNA-templated gold nanowires. There is, however, one report that quantifies the effect of nickel enhancement of nickel electrodes on the contact resistance to carbon nanotubes.[19]

Second, there is a contribution due to electron scattering in gold nanowire. It has been established by Durkan and Welland[20] that as the dimensions of a polycrystalline gold nanowire approach those of the mean free path for the electron in bulk gold (40 nm[21]) the measured resistance increases. This finding was accounted for by a model, which assumes that electrons are scattered at the surface of the wire and at the grain boundaries within the wire. This model was developed by Mayadas and Shatzkes[22,23] and was based on a related model developed by Fuchs and Sondheimer.[24,25]

Third, there is a contribution to the resistivity due to electron scattering at constrictions along the nanowire.[26] This contribution will be significant if the nanowire diameter approaches the Fermi wavelength of an electron in gold (5.5 Å).

Finally, there is a contribution to the resistivity due to electron scattering at organic or inorganic impurities in the gold nanowire. Such impurities are expected due to the use of a calf thymus DNA template, DMAP-modified gold nanoparticles, and a multicomponent enhancement solution. To the best of our knowledge, there are no reports to date that quantify the magnitude of this contribution to the measured resistance in DNA-templated gold nanowires.

After consideration of the four contributions to the measured resistance that can account for the resistivity of a DNA-templated gold nanowire, we consider each of the values reported to date.

The first resistivity we consider is that reported by Keren et al.[8] This value (2×10^{-7} Ωm, 75 nm diameter, electrodes overlaid) is close to that of bulk polycrystalline gold as might be expected for a wire on which electrodes have been overlaid and with an average diameter that is significantly greater than that of the mean free electron path in gold. Under these conditions, the contributions of contact resistance and surface scattering to the measured resistance are both expected to be small.[19,26] The fact that the resistivitiy is nevertheless higher than that of the corresponding bulk metal most likely reflects contributions from grain boundary scattering, local constrictions, and impurities to the measured resistance.

The second and third resistivities we consider are those reported by Harnack et al.[17,18] These values (2×10^{-7} Ωm, 130 nm diameter, electrodes overlaid; 3×10^{-5} Ωm, 126 nm diameter, wire overlaid) are significantly different. That this is the case is also not unexpected. In the case of the wire on which electrodes have been overlaid, the contribution of the contact resistance to the measured resistance is expected to be small. This is not expected to be the case for the wire overlaid on the electrodes, and as consequence, the resistivity is 2 orders of magnitude larger. For wires with an average diameter that is again significantly greater than that of the mean free electron path in polycrystalline gold the contributions of surface scattering to the measured resistance is expected to be small. Accordingly the resistivity of the wire on which electrodes have been overlaid is in close agreement with that reported by Keren et al.[8] and less than 1 order of magnitude larger than that of bulk polycrystalline gold. It is assumed, as above, that the reason this resistivity is higher than that for bulk polycrystalline gold is again due to electron scattering at grain boundaries, the effect of local constrictions, and the presence of impurities.

The final resistivity we consider is that reported in this paper. That this resistivity (2×10^{-4} Ωm, 30 nm diameter, wire overlaid) is higher than those discussed above is not unexpected for two reasons. First, this wire is overlaid on the electrodes. As a consequence of the resulting contact resistance, this wire is expected to possess a resistivitiy, based on the findings reported by Harnack et al.,[17,18] that is 2 orders of magnitude higher that that of bulk polycrystalline gold.[15] Second, the dimensions of this wire, being the smallest reported to date for a DNA-templated wire, are less than the mean free electron path in gold. As a consequence, the

(15) Paskaleva, A.; Atanassova, E. *Solid-State Electron.* **1998**, *42*, 777.
(16) Ford, W.; Wessels, J.; Harnack, O. Eur. Patent N1207207, 2002.
(17) Harnack, O.; Ford, W.; Yasuda, A.; Wessels, J. *Nano Lett.* **2002**, *2*, 919.
(18) Harnack, O.; Ford, W.; Karipidou, Z.; Yasuda, A.; Wessels, J. Proceedings of *Foundations of Nanoscience: Self-Assembled Architectures and Devices*; Snow Bird, Utah, USA, April 21−23, 2004.
(19) Seidel, R.; Liebau, M.; Duesburg, G.; Kreupl, F.; Unger, E.; Graham, A.; Hoenlein, W. *Nano Lett.* **2003**, *7*, 665.
(20) Durkan, C.; Welland, M. *Phys. Rev. B* **2000**, *61*, 14215.
(21) Ashcroft, A.; Mermin, N. Solid State Physics. Thesis, Saunders College, Philadelphia, 1976.
(22) Mayadas, A.; Shatzkes, M.; Janak, M. *Appl. Phys. Lett*. **1969**, *14*, 345.
(23) Mayadas, A.; Shatzkes, M. *Phys. Rev. B* **1970**, *1*, 1382.
(24) Fuchs, K.; Wills, H. *Proc. Cambridge Phil. Soc*. **1938**, *34*, 100.
(25) Sondheimer, E. *Adv. Phys*. **1952**, *1*, 1.
(26) Durkan, C.; Welland, M. *Crit. Rev. Solid State Mater. Sci.* **2000**, *25*, 1.

contribution of surface scattering to the measured resistance is expected to be large and comparable to that due to scattering of electrons at grain boundaries. This, in turn, is expected to result in an increase in the resistivity of about 1 order of magnitude. The effect of local constrictions and impurities is also expected to be significant and to account for a further increase in the resistivity of our DNA-templated gold nanowires.

Further studies are focusing on measuring the temperature-dependent resistivity of a series of nanowires overlaid on electrodes and on which electrodes have been overlaid. These nanowires have been prepared using particles of different diameters that have been enlarged to different extents. They have also been subjected to thermal, electrical, and laser annealing. By these means, the relative contributions of electron constriction, electron scattering (at grain boundaries and surfaces), and the contact resistance to the measured resistivities will be better understood.

Conclusion

We have reported the DNA-templated self-assembly of 20 nm high and 40 nm wide polycrystalline gold nanowires. These DNA-templated nanowires, the smallest reported to date, are conducting and exhibit resistivities consistent with reported findings and current theory. The use of DNA as a template for the self-assembly of conducting gold nanowires represents a potentially important approach to the fabrication of nanoscale interconnects. The challenge is to extend this approach to include the selective metallization of complex DNA architectures, enabling the DNA-templated assembly of more complex nanoscale electronic components.

Acknowledgment. This work was funded in part by the commission of the European Union (HPRN-CT-2000-0028) and by Science Foundation Ireland (CRANN CSET).

CM047970W